Detecting the Coupling Direction between both Hands Physiological Tremors – a Non-Parametric Directionality Analysis

Dobrea Monica-Claudia, Dobrea Dan-Marius
Faculty of Electronics, Telecommunication and Information Technology, "Gheorghe Asachi" Technical University, UTI, Iassy, Romania, {mcdobrea@etti.tuiasi.ro, mdobrea@etti.tuiasi.ro}

***Abstract*— This study continues some previous research done on the hand physiological tremor (PT) signal - a motor phenomenon that we treated as a potential window to better understand the dynamical structures underlying the human visuomotor circuits. In order to understand how visual inputs processing interacts with limb motor system, two intermittent light stimulation (ILS) paradigms were implemented and the corresponding dynamical evolution of limbs' motor systems outputs (i.e., the hand PTs) were tracked using a non-parametric directionality approach. In the ILS paradigms two visual stimuli, of different frequencies (7 Hz and 19 Hz), were delivered first alternatively and, then, concurrently in each of the two subjects' visual hemifields. The final results point out, at least, two major aspects: (a) the repetitive visual stimulation is not a common driver for the left and the right hand PT processes and, more, (b) the visuomotor circuits of each subject should be viewed as a distinct system, endowed with a particular responding way to the external visual stimuli.**

Keywords*— *hand physiological tremor; visual stimulation, indirect/direct coupling, non-parametric directionality analysis.

I. Introduction

The physiologic tremor, defined as rapid involuntary and, usually, unnoticed oscillations of parts of the human body [1], [2] is a motor phenomenon whose origins still continues today to arouse great interest among both the physiologists and the neuro-pathologists. As the result of interactions between neural and mechanical factors, the physiological tremor proves to be quite a complex signal, with a spectrum containing both mechanical (load dependent) and central neurogenic (load independent) components. The first type of components basically corresponds to the resonance frequencies associated with different limb segments being investigated (e. g., 15÷30 Hz for the metacarpophalangeal joint, 8÷12 Hz for the wrist; 3÷5 Hz for the elbow joints). Besides these, in the finger PT, the reported neurogenic components have proved to have frequency correspondents in both ranges of 8÷12 Hz and 30÷40 Hz [3].

In order to study the functional relation between the two central tremor oscillators, proposed in the literature [1] as controlling independently the right and the left hand PT processes, we previously used in [4] the same experimental paradigms, also presented here, together with the bivariate Granger causality analysis. The results obtained at that time did not revealed any visual influence, either at the visual stimuli frequencies or at their harmonics and/or subharmonics, in the hand PT signals; however, a significant driver, at almost 5 Hz (i.e., in the 4 ÷ 7 Hz theta band), between the two processes generating the PT signals, was uncovered. To further investigate this theta frequency bilateral coupling, a non-parametric method was adopted like that presented in [5]. With this method, that mainly estimates directionality in the bivariate data, the model validity ceases to be of concern. The concept of conditional independence was especially referred to in our paper and, together with the conditional causality measures extracted from the PT data, it helped us to investigate in what extent the particular visual stimulation was or it was not responsible, at least partially, for the theta frequency coupling revealed in [4].

II. Database and methods

A. Database

The database used for this study is the one we proposed first in [6] and, further, analyzed it in [4] and [7]. The acquisition of bilateral hand tremor signals was done using two ADXL203 low-g accelerometer sensors, a NI AT-MIO-16E-10 data acquisition board, and a new developed LabWin CVI software program. The PT signals were acquired in synchronism with the provided repetitive visual stimuli. The accelerometers and their mounting plates (with a total weight of less than 5 g each) were kept by the subjects between their middle finger and forefinger. The acquisition was done on 12 bits and the data were sampled at 240 Hz. Two different conditions (paradigms) were experimented and the bilateral PT signals were acquired from two healthy right-handed adults (i.e., one man – 32 years old, denoted in what follows by S1; one female – 29 years old, denoted by S2). All recordings took place in a quiet and dark room, with a 17 inch computer screen placed at a viewing distance of 80 cm in front of the subject. During tests, the subjects: had to visualize and focus exclusively on a white central cross shown on the screen, had to minimize both the blinking

and the stress to keep stretched their hands, in a roughly fixed horizontal position, had to avoid visual feedback and, more, had to take breaks between successive recordings in order to prevent the arm fatigue. For each subject and for each paradigm, 20 trials of 64 s each were recorded for the left and for the right hand, respectively. Two visual repetitive stimuli, of different frequencies, 7 Hz and 19 Hz, were delivered alternatively (in the 1st paradigm) or concurrently (in the 2nd paradigm) on the left and on the right half of the PC's dark screen; thus, the stimuli were supplied to the subjects in their left visual hemifield (LVH) and right visual hemifield (RVH), respectively. Placed on the imaginary "equator" line of the PC screen, the visual stimuli (i.e., circle-like flashes of white light) were delivered as follows. In the 1st paradigm, a visual stimulus was first flickered in the LVH, at a rate of 7 Hz, and only in the first 32 s of the recording (hereinafter denoted by P32); then, the second visual stimuli was provided in the RVH, at a rate of 19 Hz, and only in the last 32 s (denoted by U32). In the 2nd paradigm, in the P32 part of the recording, the both stimuli presented above (LVH–7 Hz, RVH–19 Hz) were delivered simultaneously to the subject; after that, the stimuli frequencies interchanged so that in the U32 part of the recording a stimuli delivery schema of (LVH–19 Hz, RVH–7 Hz) was applied.

B. Non-parametric Directionality Analysis

In this paper, three random processes (i.e., the left PT signal – denoted by *x*; the right PT signal – *y*; and the visual stimulation signal – referred, from now on, as the predictor signal *z*), were analyzed in order to distinguish a genuine left-right PT correlation, from an apparent or visual induced correlation. Specifically, we studied to what extent the visual input (the conditional *z* process) interacts with the limb motor system. The non-parametric conditional directionality analysis, used here, allows to examine both how coupling between the left and the right hand PTs is dependent or independent on the z process and, more, which of them is the driver. To characterize the linear pairwise interactions of the right and left hand PT signals, we estimated, in turn, the followings [5]: ***a***) the scalar measures of overall unconditional and conditional dependence, given by the squared correlation coefficient, R^2_{yx}, and the partial correlation coefficient, $R^2_{yx/z}$, respectively – see (1); ***b***) their frequency domain equivalents, namely, the coherence function, $\left|R_{yx}(\lambda)\right|^2$ and the partial coherence function, $\left|R_{yx/z}(\lambda)\right|^2$ - see (2) and (3), respectively, and **c**) the overall dependence, decomposed summatively by direction in time domain (4) and in frequency domain (5).

$$R^2_{yx} = \frac{\sigma^2_y - \sigma^2_{y|x}}{\sigma^2_y}, \quad R^2_{yx|z} = \frac{\sigma^2_{y|z} - \sigma^2_{y|x,z}}{\sigma^2_{y|z}} \qquad (1)$$

$$\left|R_{yx}(\lambda)\right|^2 = \frac{\left|f_{yx}(\lambda)\right|^2}{f_{xx}(\lambda)\cdot f_{yy}(\lambda)} \qquad (2)$$

$$\left|R_{yx|z}(\lambda)\right|^2 = \frac{\left|f_{yx|z}(\lambda)\right|^2}{f_{xx|z}(\lambda)\cdot f_{yy|z}(\lambda)} \qquad (3)$$

$$R^2_{yx|z} = R^2_{yx|z;-} + R^2_{yx|z;0} + R^2_{yx|z;+} \qquad (4)$$

$$\left|R_{yx|z}(\lambda)\right|^2 = \left|R'_{yx|z;-}(\lambda)\right|^2 + \left|R'_{yx|z;0}(\lambda)\right|^2 + \left|R'_{yx|z;+}(\lambda)\right|^2 \qquad (5)$$

In the above relations: **1**) *x* is the reference (input) process; **2**) the conditioned variances such as $\sigma^2_{y|x}$ and $\sigma^2_{y|x,z}$ (symmetrical measures which gives no information about the interaction's directionality) can be perceived as representing the variance of the error process after a linear regression of *y* on *x* and of *y* on *x* and *z*, respectively; **3**) $f_{yx}(\lambda)$ is the cross-spectrum between processes *x* and *y* (7) and $f_{xx}(\lambda)$ and $f_{yy}(\lambda)$ are the two auto-spectra; **4**) $f_{yx|z}(\lambda)$ is the partial cross-spectrum between processes *x* and *y* with predictor *z*; $f_{xx|z}(\lambda)$ and $f_{yy|z}(\lambda)$ are the two partial auto-spectra (9); **5**) the *R'* conditioned directional coherence functions are scaled, at each frequency, in compliance with the relative value of the *f'* functions (12) – for details, see [5]. All linear frequency domain parameters were estimated using methods based on the finite Fourier transform. The time series *x* and *y*, with an *R* length of 15360 samples each, were split into *L=30*, distinct non-overlapping sections of *T=512* samples. Then, for each *l* segment (*l = 1,...,L*) and each frequency λ, we computed the corresponding finite Fourier transform as:

$$d^T_x(\lambda, l) \cong \sum_{k=(l-1)T}^{lT-1} e^{-i\lambda k} x[k] \qquad (6)$$

Similar formulas were applied for the *y* and *z* signals. The two auto-spectra $f_{xx}(\lambda)$ and $f_{yy}(\lambda)$ were estimated using a formula analogous to that of the $f_{yx}(\lambda)$ cross-spectrum, given by:

$$\begin{aligned} f_{yx}(\lambda) &= \lim_{T\to\infty} \frac{1}{2\pi T} E\left\{d^T_x(\lambda)\cdot \overline{d^T_y(\lambda)}\right\} \cong \\ &\cong \frac{1}{2\pi LT}\sum_{l=1}^{L} d^T_x(\lambda, l)\cdot \overline{d^T_y(\lambda, l)} \end{aligned} \qquad (7)$$

In (7) the overbar is the complex conjugate and $E\{\}$ is the mathematical expectation. The finite Fourier transforms conditioned on a third process, *z*, were constructed as [8]:

$$d_{x|z}^T(\lambda, l) = d_x^T(\lambda, l) - \frac{f_{xz}(\lambda)}{f_{zz}(\lambda)} d_z^T(\lambda, l) \quad (l = 1,\ldots, L) \quad (8)$$

where: the quantities $f_{xz}(\lambda)$ and $f_{zz}(\lambda)$ are the cross-spectrum between the reference process *x* and the conditioning process *z* and, respectively, the auto-spectrum of *z*. From here, the partial auto-spectrum of *x* was further derived as:

$$\begin{aligned} f_{xx|z}(\lambda) \quad &= \lim_{T\to\infty} \frac{1}{2\pi T} E\left\{d_{x|z}^T(\lambda) \cdot \overline{d_{x|z}^T(\lambda)}\right\} \cong \\ &\cong \frac{1}{2\pi LT} \sum_{l=1}^{L} \left|d_{x|z}^T(\lambda, l)\right|^2 \end{aligned} \quad (9)$$

and, also, the formula for the partial coherence function as:

$$\left|R_{yx/z}(\lambda)\right|^2 = \lim_{T\to\infty} \left|corr\left\{d_y^T(\lambda) - \frac{f_{yz}(\lambda)}{f_{zz}(\lambda)} d_z^T(\lambda), d_x^T(\lambda) - \frac{f_{xz}(\lambda)}{f_{zz}(\lambda)} d_z^T(\lambda)\right\}\right|^2 \quad (10)$$

While R_{yx}^2 (1) can be viewed as that part of the variance in y that can be explained by the regressor *x*, the partial correlation coefficient, $R_{yx|z}^2$, (2) is used to reveal any common influence that process *z* may exert on both *x* and *y* processes. The coherence function, $\left|R_{yx}(\lambda)\right|^2$ (2) is a frequency domain method extensively applied to the study of neural activity [1], [2], [3], [4], [5], [6], [7], and it determines the strength of coupling, at each individual frequency, λ, between the two analyzed signals. The possible values for this function are between 0, meaning independence, and 1, denoting a signals' perfect linear relationship. Also, the partial coherence function, $\left|R_{yx/z}(\lambda)\right|^2$ was usefully applied in neurobiological studies to identify direct interactions due to common inputs in functional neural network connectivity [5]. Written as in (8), this function value can be understood as a measure of residual correlation between the x and y processes, calculated after any linear common contribution brought to them, through the z process, was removed. A value of zero for the estimates of this parameter indicates that any revealed coupling between x and y is all due to the common effect of process z.

In [5], in order to decompose, by direction, both the $R_{yx/z}^2$ scalar and the $\left|R_{yx/z}(\lambda)\right|^2$ function, the authors defined a lagged conditional correlation function between *x* and *y*, $\rho_{yx|z}(\tau)$, which is the inverse Fourier transform of the pre-whitened partial cross spectrum. Based on it, they deduced the relations (4) and (11) and, respectively, (5) and (12):

$$R_{yx}^2 = \int_{\tau<0} \left|\rho_{yx|z}(\tau)\right|^2 d\tau + \left|\rho_{yx|z}(0)\right|^2 + \int_{\tau>0} \left|\rho_{yx|z}(\tau)\right|^2 d\tau \quad (11)$$

$$f'_{yx|z;-} = \int_{\tau<0} \rho_{yx|z}(\tau)\, e^{-i\lambda\tau} d\tau \quad (12)$$

For the $f'_{yx|z;0}$ and $f'_{yx|z;+}$ functions, the integration is for $\tau = 0$ and $\tau < 0$, respectively. For more details, see [5].

III. RESULTS

All the correlation coefficients and directionality measures were obtained using Neurospec211 toolbox [5]. In Fig. 1, the results for unconditional (two processes – left and right hand PTs) and conditional (three processes – including, supplementary, the visual predictor) directional coherence functions are shown as follows: the original coherence estimate (black) with the forward (red), reverse (blue) and zero-lag (grey) components overlaid. Correspondingly, in Table 1, the scalar values for the squared correlation coefficient and for the partial correlation coefficient were calculated for different: subject (S1, S2), paradigm (P1, P2), part of the recording (T – the entire 64 s recording; P32 – the first 32 s; U32 – the last 32 s) and predictor (the *z* signal). The *M* symbol indicates that the analysis was done on the average signal obtained over the corresponding 20 recordings of each hand. The predictor signal was constructed: (**1**) as a pure sinusoidal wave of 7 or 19 Hz (i.e., the frequency of visual stimulation), denoted with the LVH/RVH marking or L/R suffix indicating the **L**eft/**R**ight Visual Hemifield predictor source (in accordance with the discussed paradigm) or (**2**) as a sum of two sinusoidal waves of 7 and 19 Hz, denoted with the LVH + RVH marking or **LR** suffix, indicating the concurrent **L**eft and **R**ight Hemifield visual stimulation (valid only for P2). For the unconditional and conditional directional coherence estimates, the 95% confidence limits for each frequency λ (shown as the dashed horizontal lines in Fig. 1) were computed as in [5], [9], based on a null hypothesis of independence or of no correlation after the common linear influences from the investigated predictor were removed, respectively.

Fig.1 (d, f, [i, k, m], [j, l, n], r, ș, [u, w, y], [v, x, z]) shows estimates of the first order partial coherence (10) between left and right PTs using distinct visual stimuli as the predictor. Comparison with the corresponding ordinary coherence estimates between left and right PTs, illustrated in Fig. 1 (c, e, g, h, q, s, t and ț, respectively), shows that the coupling around 5 Hz (and at nearly all significant coherence peaks) remains nearly unchanged in the partial coherence; this means that the significant detected left-right PTs couplings cannot be predicted by using the visual predictor signal. Moreover, **Fig. 1** (**c** *versus* **q**; **e** *versus* **s**; **g** *versus* **t**; **h** *versus* **ț**) illustrates for both S1 and S2 subjects, for both paradigms and for both P32 and U32 sub-recordings that there are not systematic changes in the pattern and direction of interaction between left and right PT processes in response (or not) to visual stimulation. The same conclusions can be drawn from comparing the corresponding S1 and S2 scalar estimates, given in Table 1, where not only the partial correlation coefficient (i.e., columns P32L/R/LR or U32L/R/LR) does not drop in comparison to the corresponding correlation

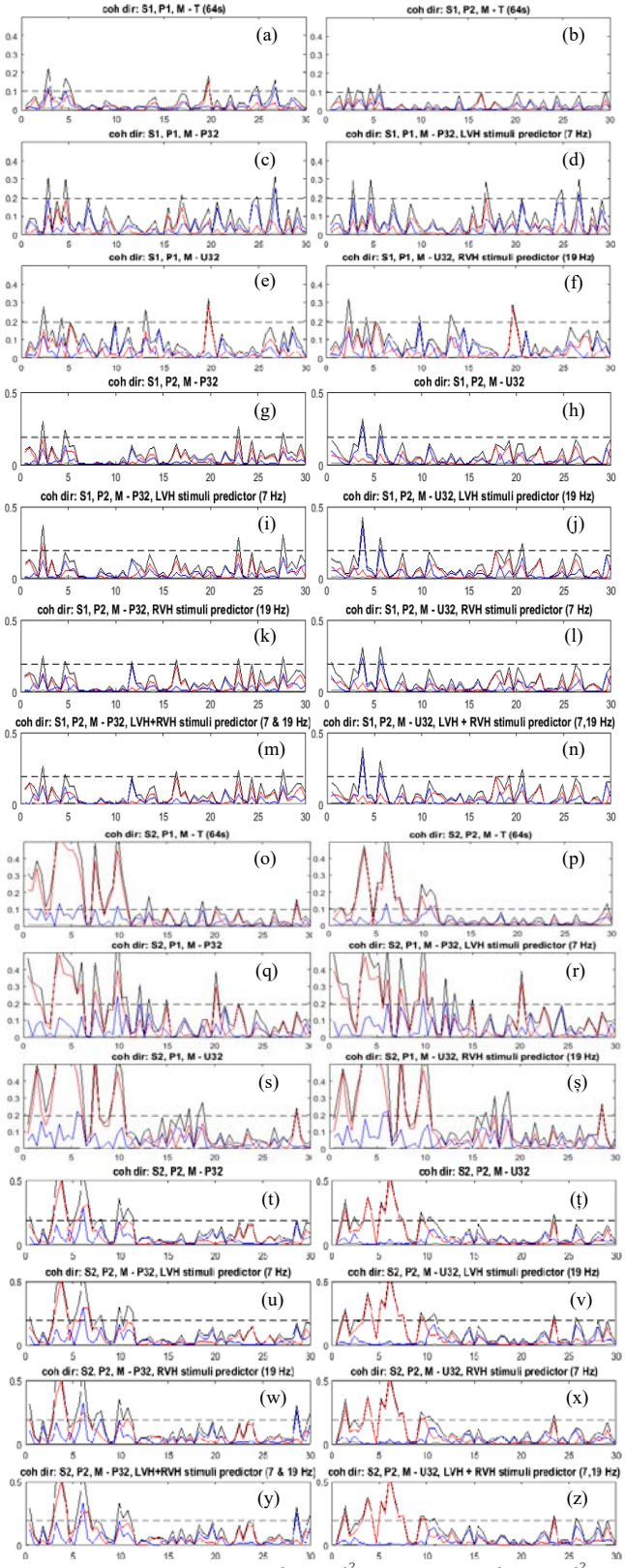

Fig. 1 Estimated unconditional, $|R_{yx}(\lambda)|^2$, and conditional, $|R_{yx/z}(\lambda)|^2$, directional coherence functions for the two subjects and the two paradigms.

TABLE I. DIRECTIONALITY METRICS CALCULATED OVER BOTH THE ENTIRE AND THE REDUCED [0, **FA**] FREQUENCY RANGE

	S1, P1					**S2, P1**				
	T M	**P32 M**	**U32 M**	**P32L (7Hz)**	**U32R (19Hz)**	**T M**	**P32 M**	**U32 M**	**P32L (7Hz)**	**U32R (19Hz)**
$\mathbf{R^2_{yx}}$	0.046	0.079	0.081	0.081	0.086	0.072	0.103	0.104	0.108	0.110
$\mathbf{R^2_{yx;\,fa}}$	0.058	0.091	0.101	0.088	0.110	0.340	0.300	0.402	0.307	0.411
$\mathbf{R^2_{yx;\,0,fa}}$	0.0047	0.0049	0.0047	0.0054	0.0055	0.0064	0.0056	0.005	0.0057	0.0054
$\mathbf{R^2_{yx;+,\,fa}}$	0.0269	0.0384	0.0553	0.0305	0.0601	0.2719	0.2370	0.3186	0.2348	0.3258
$\mathbf{R^2_{yx;-,\,fa}}$	0.0261	0.0479	0.0407	0.0517	0.0439	0.0617	0.0573	0.0784	0.0660	0.0797
$\mathbf{R^2_{yx;\,0,\,fa}(\%)}$	8.28	5.41	4.68	6.13	5.02	1.88	1.88	1.27	1.86	1.32
$\mathbf{R^2_{yx;\,+,\,fa}(\%)}$	46.59	42.12	54.92	34.84	54.88	79.96	79.01	79.22	76.60	79.28
$\mathbf{R^2_{yx;\,-,\,fa}(\%)}$	45.13	52.47	40.40	59.03	40.09	18.150	19.10	19.50	21.54	19.40

	S1, P2								**S2, P2**							
	P32_M	**U32_M**	**P32L (7Hz)**	**P32R (19 Hz)**	**P32LR (7,19Hz)**	**U32L (19 Hz)**	**U32R (7 Hz)**	**U32LR (7,19Hz**	**P32_M**	**U32_M**	**P32L (7Hz)**	**P32R (19 Hz)**	**P32LR (7,19Hz)**	**U32L (19 Hz)**	**U32R (7 Hz)**	**U32LR (7,19Hz)**
$\mathbf{R^2_{yx}}$	0.080	0.076	0.087	0.0863	0.086	0.083	0.079	0.082	0.092	0.087	0.095	0.097	0.096	0.092	0.093	0.091
$\mathbf{R^2_{yx;\,fa}}$	0.078	0.103	0.078	0.076	0.081	0.108	0.108	0.104	0.235	0.219	0.235	0.243	0.232	0.229	0.219	0.218
$\mathbf{R^2_{yx;\,0,fa}}$	0.0032	0.0051	0.0028	0.0037	0.0037	0.0056	0.0052	0.0056	0.0031	0.0054	0.0036	0.0031	0.0030	0.0048	0.0060	0.0052
$\mathbf{R^2_{yx;+,\,fa}}$	0.0507	0.0320	0.0473	0.0454	0.0474	0.0346	0.0368	0.0337	0.1632	0.1948	0.1650	0.1578	0.1552	0.2086	0.1950	0.1993
$\mathbf{R^2_{yx;-,\,fa}}$	0.0242	0.0658	0.0277	0.0270	0.0302	0.0679	0.0661	0.0645	0.0690	0.0192	0.0670	0.0824	0.0742	0.0152	0.0176	0.0140
$\mathbf{R^2_{yx;\,0,\,fa}(\%)}$	4.07	4.98	3.64	4.86	4.52	5.20	4.77	5.372	1.34	2.46	1.33	1.27	1.29	2.11	2.72	2.37
$\mathbf{R^2_{yx;\,+,\,fa}(\%)}$	64.90	31.10	60.73	59.72	58.33	31.97	34.05	32.47	69.36	88.79	70.18	64.85	66.77	91.26	89.20	91.25
$\mathbf{R^2_{yx;\,-,\,fa}(\%)}$	31.03	63.92	35.63	35.42	37.15	62.87	61.18	62.16	29.30	8.75	28.50	33.88	31.94	6.63	8.07	6.39

Note: The *fa* index is the upper frequency limit (in Hz) used for calculation of the directionality metrics. We used a value of 8 Hz in order to focus on (include and limit to) the theta frequency band that is of interest for us. The $\mathbf{R^2_{yx;\,0,\,fa}(\%)}$, $\mathbf{R^2_{yx;\,+,\,fa}(\%)}$ and $\mathbf{R^2_{yx;-,\,fa}(\%)}$ are the percentages of $\mathbf{R^2_{yx;\,fa}}$ in each direction.

coefficient (i.e., columns P32_M and, respectively, U32_M) but, more, even the leading direction of coupling is not, between the subjects, a consistent one; exactly, while in S2 the left PT process is clearly and constantly leading the right PT process (see line $\boldsymbol{R^2}_{yx;+,fa}$ (%) versus $\boldsymbol{R^2}_{yx;-,fa}$ (%)), in S1 this is no longer valid.

IV. CONCLUSIONS

In this study we have emphasized not only the influence that the visual stimuli could have on the hand tremor signal at the theta frequency (i.e., no apparent influence), but also, this research revealed the subjects' peculiarities reflected in the different way their neuronal motor circuits generate the hand PT. It is worthy to notice that the coupling between left-right hand PTs involved mainly the same frequency bands (i.e., around 5 Hz and 20-30 Hz) as those from motor unit - tremor signal and motor unit-motor unit couplings reported in [8]. More, our bilateral coherence obtained at theta frequency for the hand PTs comes to confirm the findings from [2]; in [2], the authors reported that, in PT, the two hands' oscillations are frequently mutually coherent and epochs (usually lasting from several up to a dozen seconds) of strong coherence alternate with intervals of insignificant coherence – and this, in the absence of any stimuli. This finding, in turn, comes to support our inference regarding the PT independence from the visual stimuli.

REFERENCES

[1] B. Koster, M. Lauk, J. Timmer, T. Winter, B. Guschlbauer, F. X. Glocker, A. Danek, G. Deuschl and C. H. Lucking, "Central mechanisms in human enhanced physiological tremor", Neuroscience Letter, 241 (2&3), 1998, pp. 135-138.

[2] S. Chakraborty, J. Kopecká, O. Šprdlík, M. Hoskovcová, O. Ulmanová, E. Růžička, M. Zapotocky, "Intermittent bilateral coherence in physiological and essential hand tremor", Clinical Neurophysiology, 128, 2017, pp. 622–634

[3] D.M. Halliday, B.A. Conway, S.F. Farmer, and J.R. Rosenberg, "Load-Independent Contributions From Motor-Unit Synchronization to Human Physiological Tremor", Journal of Neurophysiology, 82(2), 1999, pp. 664-675

[4] M.-C. Dobrea, D.M. Dobrea, "Central tremor oscillators – a directionality study", INISTA 2007 International Symposium on Innovations in Intelligent Systems and Applications, Istanbul, Turkey, 2007, pp. 91-95

[5] D. M. Halliday, M. H. Senik, C. W. Stevenson, R. Mason, "Non-parametric directionality analysis – Extension for removal of a single common predictor and application to time series", Journal of Neuroscience Methods, 268, 2016, pp. 87-97.

[6] M.-C. Serban, D.M. Dobrea, "Central Physiological Tremor Oscillators within a Hemifield Repetitive Visual Stimulation Paradigm", 28th Annual International Conference of the IEEE Engineering in Medicine and Biology Society, New York, SUA, 2006, vols. 1-15, pp. 2780-2783.

[7] M.-C. Serban, D.M. Dobrea, "Postural Hand Tremor and the Repetitive Photic Stimulation – A Coherence Joint Time Frequency Study", World Congress on Medical Physics and Biomedical Engineering 2006. IFMBE Proceedings, vol 14/2 Springer, Berlin, pp. 987-991

[8] D.R. Brillinger,"Some statistical methods for random process data from seismology and neurophysiology", Ann. Stat., 16, 1988, pp. 1–54.

[9] D. M. Halliday, J. R. Rosenberg , A. M. Amjad, P. Breeze, , B. A. Conway, and S. F. Farmer, "A framework for the analysis of mixed time series/point process data—theory and application to the study of physiological tremor, single motor unit discharges and electromyograms", Progress in Biophysics and Molecular Biology, 64, 1995, pp. 237–278